Assembling an isomer grid: the isomorphous 4-, 3- and 2-fluoro-N′-(4-pyridyl)benzamides

Katie Donnelly,[a] John F. Gallagher[a]* and Alan J. Lough[b]

[a]School of Chemical Sciences, Dublin City University, Dublin 9, Ireland, and
[b]Department of Chemistry, 80 St George Street, University of Toronto, Ontario, Canada M5S 3H6

Correspondence e-mail: john.gallagher@dcu.ie

The three title isomers, 4-, (I), 3-, (II), and 2-fluoro-N′-(4-pyridyl)benzamide, (III), all $C_{12}H_9FN_2O$, crystallize in the $P2_1/c$ space group (No. 14) with similar unit-cell parameters and are isomorphous and isostructural at the primary hydrogen-bonding level. An intramolecular C—H···O=C interaction is present in all three isomers [C···O = 2.8681 (17)–2.884 (2) Å and C—H···O117–118°], with an additional N—H···F [N···F = 2.7544 (15) Å] interaction in (III). Intermolecular amide–pyridine N—H···N hydrogen bonds link molecules into one-dimensional zigzag chains [graph set $C(6)$] along the [010] direction as the primary hydrogen bond [N···N = 3.022 (2), 3.049 (2) and 3.0213 (17) Å]. These are augmented in (I) by C—H···π(arene) and cyclic C—F···π(arene) contacts about inversion centres, in (II) by C—F···F—C interactions [C···F = 3.037 (2) Å] and weaker C—H···π(arene)/C—H···F contacts, and in (III) by C—H···π(arene) and C=O···O=C interactions, linking the alternating chains into two-dimensional sheets. Typical amide N—H···O=C hydrogen bonds [as $C(4)$ chains] are not present [N···O = 3.438 (2) Å in (I), 3.562 (2) Å in (II) and 3.7854 (16) Å in (III)]; the C=O group is effectively shielded and only participates in weaker interactions/contacts. This series is unusual as the three isomers are isomorphous (having similar unit-cell parameters, packing and alignment), but they differ in their interactions and contacts at the secondary level.

Comment

Structural systematics of small molecules has undergone an enormous change in the past decade with technical advances in the ability to collect and analyse many crystal structures within a short timeframe. Of interest in this research are studies on polymorphism, pseudopolymorphism and isomers and their impact on the development of new materials (Gelbrich et al., 2007; Wardell et al., 2007, 2008). As progress in predicting crystal structures continues to greatly expand knowledge from first principles, it is the drive amongst synthetic chemists and chemical crystallographers to assemble comprehensive sets of crystal structure data that will provide a continual challenge to but also aid in the ongoing development of this predictive science (Day et al., 2005). A relatively facile method of obtaining extensive and related crystal structure data sets is the assembly of isomer grids and subsequent grid expansion (with polymorphs of individual compounds), using variable solvent content and cocrystallizations to generate pseudopolymorphs, and using variable-temperature studies to analyse potential phase changes. We report here the molecular and crystal structures of the 4-, 3- and 2-fluoro-N′-(4-pyridyl)benzamide isomers, (I)–(III) (Figs. 1–3), obtained from the reaction of 4-, 3- and 2-fluorobenzoyl chloride and 4-aminopyridine. This is the first in a series of studies of isomers and model compounds for the assembly of an isomer grid.
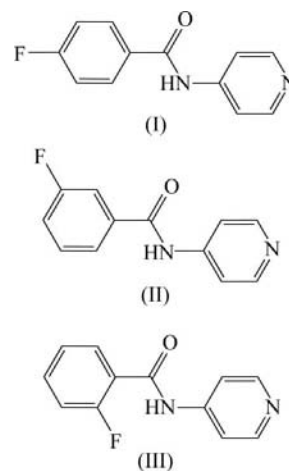
The geometric data (bond lengths and angles) in (I)–(III) are normal and are not discussed except for some comparisons and with reference to the hydrogen bonding. It is of note that the C—F bond lengths differ markedly [1.365 (2) Å in (I), 1.354 (2) Å (II) and 1.3451 (16) Å (III)], probably as a result of the secondary hydrogen bonding (see below). The F atom is located cisoid to the C=O group in (II) but transoid in (III).
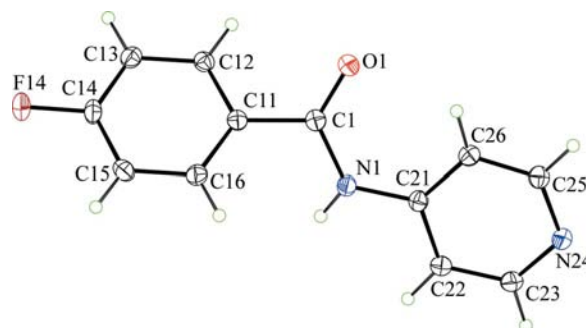

Figure 1
A view of (I), showing the atomic numbering scheme. Displacement ellipsoids are drawn at the 30% probability level.

organic compounds

No noticeable trends are evident from analysis of the bond-angle data. The defining feature of the molecular conformation is the benzene–pyridine dihedral angle, which is mutually oriented at 51.95 (6)° in (I), 48.75 (6)° in (II) and 46.34 (5)° (III) (see the torsion angles in Tables 1, 3 and 5); pyramida-
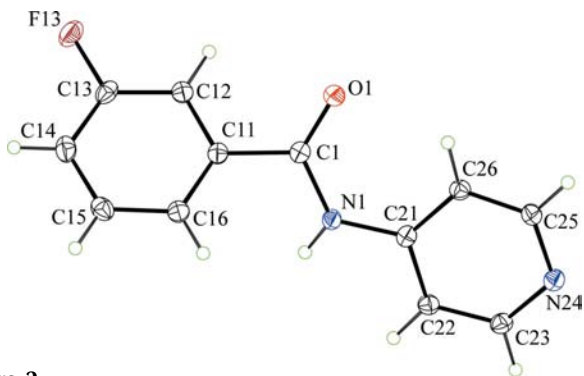

Figure 2
A view of (II), showing the atomic numbering scheme. Displacement ellipsoids are drawn at the 30% probability level.
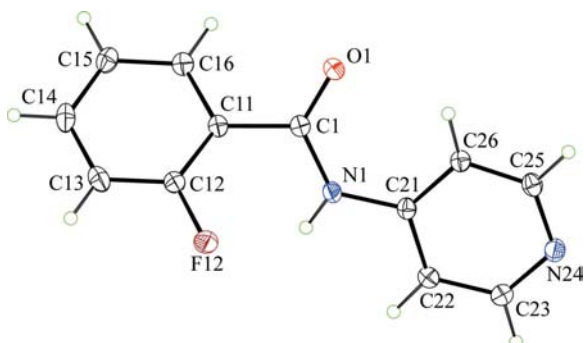

Figure 3
A view of (III), showing the atomic numbering scheme. Displacement ellipsoids are drawn at the 30% probability level.
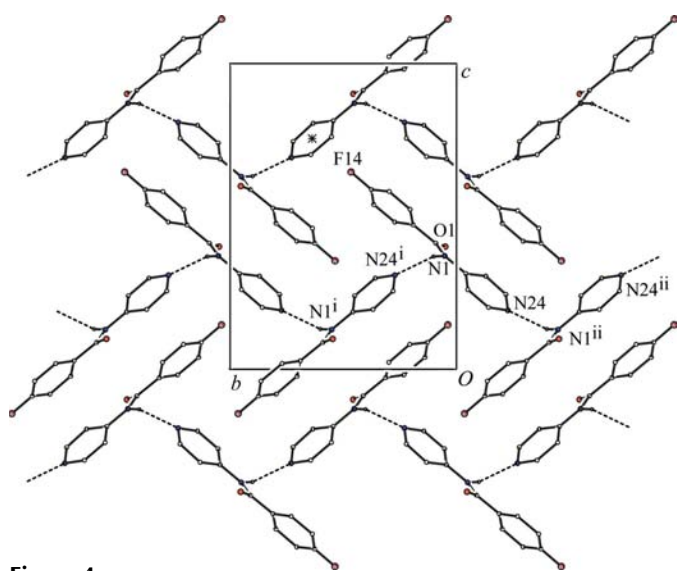

Figure 4
The primary N—H···N interactions in (I); H atoms not involved in hydrogen bonding have been omitted for clarity. The pyridine ring at position $(x, -y + \frac{1}{2}, z + \frac{1}{2})$ [labelled with an asterisk (*)] participates in an F···π(arene) contact. [Symmetry codes: (i) $-x + 1, y + \frac{1}{2}, -z + \frac{1}{2}$; (ii) $-x + 1, y - \frac{1}{2}, -z + \frac{1}{2}$.]

lization is not discernible at the amide N1 atom, with angles summing to within 3° of 360°.

For molecular comparisons, the asymmetric units have been chosen to be close to the origin and with the molecular axes aligned in similar orientations. A key feature in all three isomers is the intramolecular interaction between atoms C26 and O1 [with an $S(6)$ motif], with C26···O1 in the narrow range of 2.87 ± 0.01 Å. In (III), there is an additional intramolecular N—H···F interaction [N···F = 2.7544 (15) Å] between the *ortho*-F and amide NH atoms (see Tables 2, 4 and 6).

The defining and primary intermolecular interaction in all three systems is the amide–pyridine N—H···N hydrogen bond that links molecules into one-dimensional zigzag chains [graph set $C(6)$] along the [010] direction [with N···N distances of 3.022 (2), 3.049 (2) and 3.0213 (17) Å].
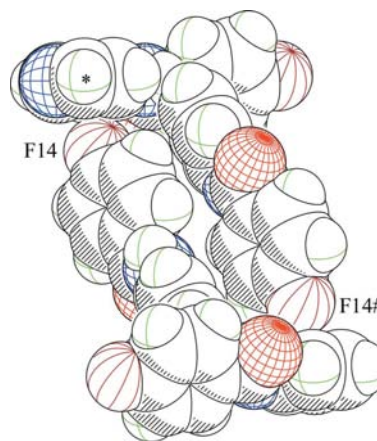

Figure 5
A view of the packing and C—F···π(arene) contacts in (I), with atoms depicted as their van der Waals spheres. The hash symbol (#) denotes an inversion-symmetry-related molecule at position $(-x + 2, -y, -z + 1)$. The asterisk (*) indicates the pyridine ring defined in Fig. 4.
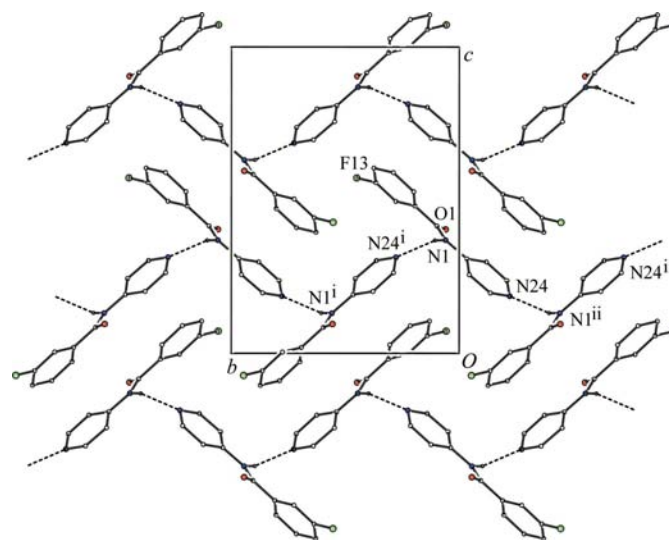

Figure 6
The primary N—H···N interactions in (II); H atoms not involved in these interactions have been omitted. [Symmetry codes: (i) $-x + 1, y + \frac{1}{2}, -z + \frac{1}{2}$; (ii) $-x + 1, y - \frac{1}{2}, -z + \frac{1}{2}$.]

In (I), weaker C—H⋯π(arene) and C—F⋯π(arene) contacts (about inversion centres) link alternating chains into a two-dimensional sheet [Table 2; F14⋯C21^{v} = 3.091 (2) Å; symmetry code: (v) x, $-y + \frac{1}{2}$, $z + \frac{1}{2}$], with each chain dovetailing into its two nearest neighbouring chains aligned in the opposite direction along [010] (Figs. 4 and 5). There are no C—H⋯F—C or C—F⋯F—C interactions.

In (II), the primary interaction is augmented by three weaker C—H⋯π(arene) contacts per molecule, linking the alternating chains into a two-dimensional sheet (Table 4); each chain dovetails as in (I) (Figs. 6 and 7). Instead of C—F⋯π(arene) facial contacts as for (I), the location of the F atom provides alternative interaction sites. The most notable is the C13—F13⋯(F13–C13)^{vi} contact about an inversion centre [F13⋯C13^{vi} = 3.037 (2) Å and F13⋯F13^{vi} = 3.1180 (17) Å; symmetry code: (vi) $-x + 2$, $-y + 1$, $-z + 1$], with an offset C_6 interplanar separation of 3.01 Å. Two weak C—H⋯F contacts are also present (H⋯F = 2.65 Å, and C—H⋯F = 115 and 117°).

In (III), the one-dimensional chains are further linked by C—H⋯π(arene) contacts into two-dimensional sheets (Figs. 8 and 9, and Table 6). Molecules are also linked via antiparallel C=O⋯O=C interactions (Allen et al., 1998) aligned about inversion centres, with C1⋯O1^{iii} distances of 3.1919 (16) Å [symmetry code: (iii) $-x + 2$, $-y$, $-z + 1$].

Usually benzamides form intermolecular N—H⋯O=C interactions [with a $C(4)$ graph set] as their primary interaction in the absence of other competing strong donors/acceptors (Gowda et al., 2008). In (I)–(III), the amide NH group and pyridine N-atom acceptor form amide–pyridine N—H⋯N chains [graph set $C(6)$] as the primary interaction, thus preventing the formation of standard $C(4)$ chains. In (I), the closest intermolecular N⋯O contact [N1⋯O1($x - 1$, y, z) = 3.438 (2) Å along [100]; N—H⋯O = 125°] is 0.4 Å longer and ∼20° smaller in angle than the amide–pyridine N—H⋯N interaction. For (II), the closest intermolecular N⋯O contact [N1⋯O1($x - 1$, y, z) = 3.562 (2) Å along [100]; N—H⋯O = 130°] is 0.5 Å longer and ca 18° smaller in angle than the amide–pyridine N—H⋯N interaction, while in (III) the

closest intermolecular N⋯O contact [N1⋯O1($x - 1$, y, z) = 3.7854 (16) Å along [100]; N—H⋯O = 135°] is ∼0.75 Å longer and ca 4° smaller in angle than the amide–pyridine N—H⋯N interaction.

All three isomers have similar unit-cell parameters in the monoclinic space group $P2_1/c$ (No. 14), and have similar packing and hydrogen-bond motifs (similar at the primary level but different at the secondary interaction levels), and they are isomorphous (in the strict interpretation of the definition, as the atom-site coordinates coincide) in the solid state. The close similarity in the packing of all three structures is relatively easy to visualize (Figs. 4, 6 and 8 display three zigzag chains with the unit-cell axes). For comparison, the unit-cell similarity index, Π, is less than 0.015 for the (I)/(II)/(III) pairs (Kálmán et al., 1993); homeostructural crystal pairs and packing 'similarities' generated by substituent migration in dichloroanilines have also been discussed by Dou et al. (1993) and Kálmán et al. (1993).
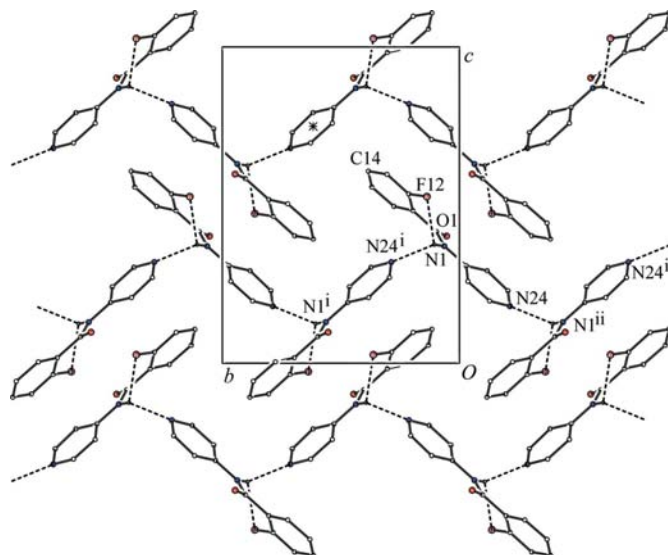

Figure 8
The primary N—H⋯N interactions in (III); H atoms not involved in these interactions have been omitted. The asterisk (*) indicates the symmetry-related pyridine ring at (x, $y - \frac{1}{2}$, $z + \frac{1}{2}$). [Symmetry codes: (i) $-x + 1$, $y + \frac{1}{2}$, $-z + \frac{1}{2}$; (ii) $-x + 1$, $y - \frac{1}{2}$, $-z + \frac{1}{2}$.]
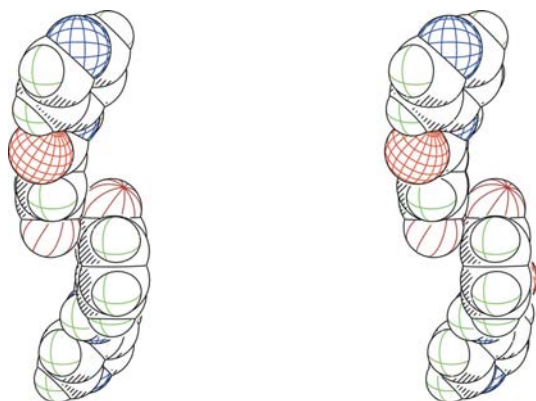

Figure 7
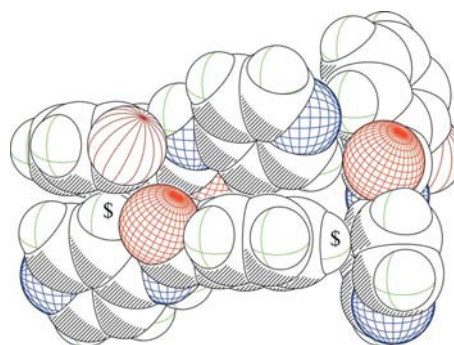A stereoview of the C—F⋯F—C contacts in (II), with atoms depicted as their van der Waals spheres.

Figure 9
Two C—H⋯π(arene) contacts in (III), with atoms depicted as their van der Waals spheres; the dollar symbols ($) indicate the arene rings.

organic compounds

The replacement of an F atom on the C_6 ring involves isosteric replacement of an H atom. The change of the F-atom site from *para* to *meta* to *ortho* only generates different secondary interactions (as can be reasoned), as primary amide–pyridine N—H···N interactions define the principal aggregation mode. Chopra & Row (2008) have recently reported a comprehensive study on a series of mono- and difluorobenzanilides [DC3–DC1, hereafter denoted DC(3–1); see scheme below]. The DC(3–1) structures correspond to (I)–(III) by replacement of the pyridine N atom by a CH group. The DC(3–1) packing is dominated by standard N—H···O=C hydrogen bonds [3.165 (4)–3.254 (4) Å], the intramolecular C_6/C_6 plane angles range from 23.0 (3) to 32.9 (1)°, and the N···O distances are at least 0.2 Å shorter than the corresponding data in (I)–(III) (Chopra & Row, 2008). In these fluorobenzanilides, alteration of the packing modes is observed as the F-atom position changes through *para* to *meta* to *ortho*. In related work, Gowda *et al.* (2008) have also reported a series of similar substituted alkyl- and chlorophenylbenzamides. Wardell *et al.* (2008) have also recently reported an extensive series of *N*-arylpyrazinecarboxamides; however, the authors state that isomeric compounds in this series 'show little resemblance in the supramolecular behaviour beyond crystallization in the same space group'. Clearly, more expanded isomer series are needed for detailed structural and computational comparisons.
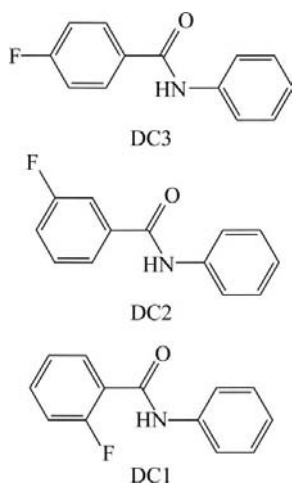
Melting-point analysis and correlations with structural properties have been reviewed for organic compounds by several groups recently (Slovokhotov *et al.*, 2004; Gilbert, 2007). Researchers have noted that more symmetrical structural isomers almost always possess higher melting points than their less symmetric analogues (Gilbert, 2007). Compounds (I)–(III) can only possess mirror symmetry (C_s) as the highest possible molecular symmetry in the appropriate conformation (solution/gas phase), but for (III) this is unlikely on steric grounds (N—H···F steric hindrance). There is a distinct trend from (I) (456–459 K) to (II) (443–446 K) to (III) (396–398 K).

The overall packing is very similar at the primary amide–pyridine N—H···N level and reasonably comparable (in terms of the number and type of weak interactions) at the secondary level.

An explanation for this melting-point trend may be the distinct N—H···O=C distance differences of 3.438 (2), 3.562 (2) and 3.7854 (16) Å in (I)–(III), resulting from the molecular packing; the packing may be such as to prevent the potential (though temporary) formation of amide–amide N—H···O=C interactions as the amide–pyridine N—H···N interactions weaken on heating. In (I), without the steric demand of an *ortho*-F atom, the weakening of the amide–pyridine N—H···N hydrogen bond may be compensated for and offset by some increasing but temporary N—H···O=C interaction, resulting in the observed melting-point trend.

The present series is unusual as the three isomers are isomorphous (having similar unit-cell parameters, packing and alignment), but differ in F/H peripheral atom-site position and in their interactions and contacts at the secondary level.

Experimental

For the preparation of (I)–(III), typically, 4-/3-/2-fluorobenzoyl chloride in dry CH_2Cl_2 (20–30 ml) was added dropwise (over a period of 2–3 min) to a 20–30 ml solution of 4-aminopyridine containing Et_3N (1.5 ml), and the reaction mixture was stirred overnight. Typical organic work-up and washing furnished the products in reasonable yields of 20–40%. Crystals suitable for X-ray diffraction were grown from $CHCl_3$ as colourless blocks over a period of 1–2 weeks.

For (I), m.p. 456–459 K (uncorrected). IR ($\nu_{C=O}$, cm^{-1}): 1723 (*s*), 1682 (*m*) (CHCl$_3$); 1677 (*s*) (KBr). ^{1}H NMR (400 MHz, CDCl$_3$): δ 8.47 (*d*, 2H, 4-pyr), 8.07 (*br s*, 1H, N—H), 7.84 (*m*, 2H, 4-Fbenz), 7.54 (*d*, 2H, 4-pyr), 7.12 (*m*, 2H, 4-Fbenz). For (II), m.p. 443–446 K (uncorrected). IR ($\nu_{C=O}$, cm^{-1}): 1738 (*w*), 1710 (*s*) (CHCl$_3$); 1683 (*s*) (KBr). ^{1}H NMR (as above): δ 8.60 (*d*, 2H, 4-pyr), 7.93 (*br s*, 1H, N—H), 7.64 (*m*, 4H, 4-pyr and 3-Fbenz), 7.53 (*m*, 1H, 3-Fbenz), 7.35 (*m*, 1H, 3-Fbenz). For (III), m.p. 396–398 K (uncorrected). IR ($\nu_{C=O}$, cm^{-1}): 1689 (*s*) (CHCl$_3$); 1685 (*s*) (KBr). ^{1}H NMR (as above): 8.66 (*br d*, 1H, N—H), 8.57 (*d*, 2H, 4-pyr), 8.17 (*t*, 1H, 2-FBenz), 7.64 (*m*, 2H, 4-pyr), 7.59 (*m*, 1H, 2-Fbenz), 7.36 (*t*, 1H, 2-Fbenz), 7.22 (*t*, 1H, 2-Fbenz).

Isomer (I)

Crystal data

$C_{12}H_9FN_2O$	$V = 988.27$ (10) Å^3
$M_r = 216.21$	$Z = 4$
Monoclinic, $P2_1/c$	Mo $K\alpha$ radiation
$a = 5.6506$ (3) Å	$\mu = 0.11$ mm^{-1}
$b = 11.3882$ (8) Å	$T = 150$ (1) K
$c = 15.4314$ (8) Å	$0.26 \times 0.14 \times 0.12$ mm
$\beta = 95.602$ (3)°	

Data collection

Nonius KappaCCD diffractometer	7401 measured reflections
Absorption correction: multi-scan	2246 independent reflections
(*SORTAV*; Blessing, 1995)	1465 reflections with $I > 2\sigma(I)$
$T_{min} = 0.893$, $T_{max} = 0.988$	$R_{int} = 0.052$

Refinement

$R[F^2 > 2\sigma(F^2)] = 0.051$	H atoms treated by a mixture of
$wR(F^2) = 0.147$	independent and constrained
$S = 1.03$	refinement
2246 reflections	$\Delta\rho_{max} = 0.28$ e Å^{-3}
149 parameters	$\Delta\rho_{min} = -0.31$ e Å^{-3}

Table 1
Selected torsion angles (°) for (I).

O1—C1—N1—C21	2.5 (3)	C11—C1—N1—C21	−178.28 (16)
O1—C1—C11—C12	32.0 (2)	C1—N1—C21—C26	17.7 (3)

Table 2
Hydrogen-bond geometry (Å, °) for (I).

$Cg1$ is the centroid of the C11–C16 ring.

D—H$\cdots A$	D—H	H$\cdots A$	$D\cdots A$	D—H$\cdots A$
N1—H1$\cdots$N24^i	0.84 (2)	2.29 (2)	3.022 (2)	146 (2)
C26—H26$\cdots$O1	0.95	2.32	2.878 (2)	117
C26—H26$\cdots Cg1^{ii}$	0.95	2.71	3.373 (2)	128

Symmetry codes: (i) $-x + 1, y + \frac{1}{2}, -z + \frac{1}{2}$; (ii) $-x + 2, -y, -z + 1$.

Isomer (II)

Crystal data

$C_{12}H_9FN_2O$	$V = 978.45$ (8) Å^3
$M_r = 216.21$	$Z = 4$
Monoclinic, $P2_1/c$	Mo $K\alpha$ radiation
$a = 5.7537$ (3) Å	$\mu = 0.11$ mm^{-1}
$b = 11.2421$ (4) Å	$T = 150$ (2) K
$c = 15.1672$ (7) Å	$0.32 \times 0.20 \times 0.12$ mm
$\beta = 94.188$ (2)°	

Data collection

Nonius KappaCCD diffractometer	8753 measured reflections
Absorption correction: multi-scan	2236 independent reflections
(*SORTAV*; Blessing, 1995)	1474 reflections with $I > 2\sigma(I)$
$T_{min} = 0.801$, $T_{max} = 0.989$	$R_{int} = 0.054$

Refinement

$R[F^2 > 2\sigma(F^2)] = 0.048$	H atoms treated by a mixture of
$wR(F^2) = 0.132$	independent and constrained
$S = 1.06$	refinement
2236 reflections	$\Delta\rho_{max} = 0.26$ e Å^{-3}
150 parameters	$\Delta\rho_{min} = -0.28$ e Å^{-3}

Table 3
Selected torsion angles (°) for (II).

O1—C1—N1—C21	5.4 (3)	C11—C1—N1—C21	−175.38 (15)
O1—C1—C11—C12	31.8 (2)	C1—N1—C21—C26	13.8 (3)

Table 4
Hydrogen-bond geometry (Å, °) for (II).

$Cg1$ and $Cg2$ are the centroids of the C11–C16 and C21–C23/N24/C25/C26 rings.

D—H$\cdots A$	D—H	H$\cdots A$	$D\cdots A$	D—H$\cdots A$
N1—H1$\cdots$N24^i	0.847 (19)	2.30 (2)	3.049 (2)	147.6 (16)
C26—H26$\cdots$O1	0.95	2.31	2.884 (2)	118
C26—H26$\cdots Cg1^{ii}$	0.95	2.78	3.4407 (18)	128
C14—H14$\cdots Cg2^{iii}$	0.95	2.88	3.808 (2)	165
C15—H15$\cdots Cg2^{iv}$	0.95	2.83	3.505 (2)	129

Symmetry codes: (i) $-x + 1, y + \frac{1}{2}, -z + \frac{1}{2}$; (ii) $-x + 2, -y, -z + 1$; (iii) $x, -y - \frac{1}{2}, z - \frac{1}{2}$; (iv) $-x + 1, -y, -z + 1$.

Isomer (III)

Crystal data

$C_{12}H_9FN_2O$	$V = 989.80$ (8) Å^3
$M_r = 216.21$	$Z = 4$
Monoclinic, $P2_1/c$	Mo $K\alpha$ radiation
$a = 5.9832$ (3) Å	$\mu = 0.11$ mm^{-1}
$b = 11.1508$ (5) Å	$T = 150$ (2) K
$c = 14.8921$ (7) Å	$0.35 \times 0.30 \times 0.18$ mm
$\beta = 94.986$ (3)°	

Data collection

Nonius KappaCCD diffractometer	6092 measured reflections
Absorption correction: multi-scan	2252 independent reflections
(*SORTAV*; Blessing, 1995)	1744 reflections with $I > 2\sigma(I)$
$T_{min} = 0.911$, $T_{max} = 0.982$	$R_{int} = 0.031$

Refinement

$R[F^2 > 2\sigma(F^2)] = 0.044$	H atoms treated by a mixture of
$wR(F^2) = 0.121$	independent and constrained
$S = 1.04$	refinement
2252 reflections	$\Delta\rho_{max} = 0.18$ e Å^{-3}
149 parameters	$\Delta\rho_{min} = -0.24$ e Å^{-3}

Table 5
Selected torsion angles (°) for (III).

O1—C1—N1—C21	6.1 (2)	C11—C1—N1—C21	−176.77 (12)
O1—C1—C11—C12	−147.55 (14)	C1—N1—C21—C26	11.2 (2)

Table 6
Hydrogen-bond geometry (Å, °) for (III).

$Cg1$ and $Cg2$ are the centroids of the C11–C16 and C21–C23/N24/C25/C26 rings.

D—H$\cdots A$	D—H	H$\cdots A$	$D\cdots A$	D—H$\cdots A$
N1—H1$\cdots$N24^i	0.844 (19)	2.333 (18)	3.0213 (17)	139.1 (15)
N1—H1$\cdots$F12	0.844 (19)	2.342 (17)	2.7544 (15)	110.6 (14)
C26—H26$\cdots$O1	0.95	2.30	2.8681 (17)	118
C26—H26$\cdots Cg1^{ii}$	0.95	2.83	3.4549 (13)	124
C14—H14$\cdots Cg2^{iii}$	0.95	2.93	3.7693 (17)	149

Symmetry codes: (i) $-x + 1, y + \frac{1}{2}, -z + \frac{1}{2}$; (ii) $-x + 2, -y, -z + 1$; (iii) $x, -y - \frac{1}{2}, z - \frac{1}{2}$.

H atoms attached to C atoms were treated as riding using the *SHELXL97* (Sheldrick, 2008) defaults at 150 (1) K [C—H = 0.95 Å and $U_{iso}(H) = 1.2U_{eq}(C)$]; N-bound H atoms were refined freely with isotropic displacement parameters to bond lengths of 0.84 (2) Å in (I), 0.847 (19) Å in (II) and 0.844 (19) Å in (III).

organic compounds

Supplementary data for this paper are available from the IUCr electronic archives (Reference: SK3227). Services for accessing these data are described at the back of the journal.

References

Allen, F. H., Baalham, C. A., Lommerse, J. P. M. & Raithby, P. R. (1998). *Acta Cryst.* B**54**, 320–329.
Blessing, R. H. (1995). *Acta Cryst.* A**51**, 33–38.
Chopra, D. & Guru Row, T. N. (2008). *CrystEngComm*, **10**, 54–67.
Day, G. M., Motherwell, W. D. S., Ammon, H. L., Boerrigter, S. X. M., Della Valle, R. G., Venuti, E., Dzyabchenko, A., Dunitz, J. D., Schweizer, B., van Eijck, B. P., Erk, P., Facelli, J. C., Bazterra, V. E., Ferraro, M. B., Hofmann, D. W. M. *et al.* (2005). *Acta Cryst.* B**61**, 511–527.
Dou, S., Weiden, N. & Weiss, A. (1993). *Acta Chim. Acad. Sci. Hung.* **130**, 497–522.
Ferguson, G. (1998). *PREP8*. University of Guelph, Canada.
Gelbrich, T., Hursthouse, M. B. & Threlfall, T. L. (2007). *Acta Cryst.* B**63**, 621–632.
Gilbert, A. S. (2007). *Thermochim. Acta*, **452**, 135–139.
Gowda, B. T., Tokarčík, M., Kožíšek, J. & Sowmya, B. P. (2008). *Acta Cryst.* E**64**, o83.
Kálmán, A., Párkányi, L. & Argay, G. (1993). *Acta Cryst.* B**49**, 1039–1049.
Lu, S.-Y., Hong, J. & Pike, V. W. (2003). *J. Labelled Compd Radiopharm.* **46**, 1249–1259.
McArdle, P. (1995). *J. Appl. Cryst.* **28**, 65.
Nonius (1997). *KappaCCD Server Software*. Windows 3.11 Version. Nonius BV, Delft, The Netherlands.
Otwinowski, Z. & Minor, W. (1997). *Methods in Enzymology*, Vol. 276, *Macromolecular Crystallography*, Part A, edited by C. W. Carter Jr & R. M. Sweet, pp. 307–326. New York: Academic Press.
Sakakibara, K., Yoneshima, N. & Osawa, T. (1987). Jpn Kokai Tokkyo Koho, CODEN JKXXAF JP 62158252 A 19870714 Showa (patent written in Japanese).
Sheldrick, G. M. (2008). *Acta Cryst.* A**64**, 112–122.
Slovokhotov, Y. L., Neretin, A. S. & Howard, J. A. K. (2004). *New J. Chem.* **28**, 967–979.
Spek, A. L. (2003). *J. Appl. Cryst.* **36**, 7–13.
Wardell, S. M. S. V., de Souza, M. V. N., Vasconcelos, T. R. A., Ferreira, M. L., Wardell, J. L., Low, J. N. & Glidewell, C. (2008). *Acta Cryst.* B**64**, 84–100.
Wardell, S. M. S. V., de Souza, M. V. N., Wardell, J. L., Low, J. N. & Glidewell, C. (2007). *Acta Cryst.* B**63**, 879–895.